Black humic acid dynamics during natural reforestation of Japanese pampas grass (Miscanthus sinensis)

著者別名	田村 憲司, 東 照雄
journal or publication title	Soil biology and biochemistry
volume	57
page range	60-67
year	2013-02
権利	(C) 2012 Elsevier Ltd. NOTICE: this is the author's version of a work that was accepted for publication in Soil biology and biochemistry. Changes resulting from the publishing process, such as peer review, editing, corrections, structural formatting, and other quality control mechanisms may not be reflected in this document. Changes may have been made to this work since it was submitted for publication. A definitive version was subsequently published in Soil biology and biochemistry [VOL57 (February 2013)] DOI : 10.1016/j.soilbio.2012.07.011.
URL	http://hdl.handle.net/2241/119285

doi: 10.1016/j.soilbio.2012.07.011

Research Paper

Black humic acid dynamics during natural reforestation of Japanese pampas grass (*Miscanthus sinensis*)

Yasuo Iimura [a,1], Mari Fujimoto [a], Kenji Tamura [b], Teruo Higashi [b], Miyuki Kondo [c], Masao Uchida [c], Koyo Yonebayashi [d], Nobuhide Fujitake [a,*]

[a] *Graduate School of Agricultural Science, Kobe University, 1-1 Rokkodai, Nada, Kobe, 657-8501, Japan*

[b] *Graduate School of Life and Environmental Sciences, University of Tsukuba, 1-1-1 Ten-noudai, Tsukuba, 305-8572, Japan*

[c] *NIES-TERRA AMS facility, National Institute for Environmental Studies (NIES), 16-2 Onogawa, Tsukuba 305-8506, Japan*

[d] *Environmental Sciences, Ishikawa Prefectural University, 1-308 Nonoichi, Ishikawa, 921-8836, Japan*

* Corresponding author. Tel./fax: +81 78 803 5847.

E-mail address: fujitake@kobe-u.ac.jp (N. Fujitake).

[1] Present address: River Basin Research Center, Gifu University, 1-1 Yanagido, Gifu 501-1193, Japan.

ABSTRACT

The dynamics of the polyaromatic structures of black humic acids (HAs), which are presumably derived from charred materials, are of significant interest for the global carbon cycle. However, the details of those dynamics are not yet well understood. We investigated differences in the degree of darkness (A_{600}/C values), isotopic ratios ($\delta^{13}C$, $\delta^{15}N$, and $\Delta^{14}C$ values), and ^{13}C NMR spectra of size-separated black HAs extracted from Japanese volcanic ash soils in order to estimate the variations in the polyaromatic structures of black HAs during ca. 100 years of natural reforestation of Japanese pampas grassland. For several hundred years, all the study sites were managed similarly as grassland by burning. Subsequently, their management differed: at site G (*Miscanthus sinensis*: C4 plant), maintenance as of the time of this study was still performed by mowing, while at sites P (*Pinus densiflora*: C3 plant) and Q (*Quercus crispula*: C3 plant), maintenance was discontinued ca. 30 and 100 years ago, respectively. Thus, the sites range from grassland (site G) to coniferous forest (site P) to broad-leaved forest (site Q). For all HA size fractions at all sites, we found that $\delta^{13}C$ values correlate positively with $\delta^{15}N$ values, although the gradients are much lower for fractions of small to medium molecular size than for fractions of medium to large molecular size (denoted as *lower-size* and *higher-size* fractions, respectively). Overall, for the lower-size fractions, the contribution ratio of C4-plant-derived carbon shows a significant positive correlation with A_{600}/C values and a negative correlation with $\Delta^{14}C$ values, and their aromatic characteristics are greater than those of higher-size fractions within the same black HA. Furthermore, the relative proportion of lower-size fractions

decreases with reforestation, especially from site P to Q. The $\delta^{13}C$ values for all size fractions are similar for sites G and P, but are relatively low for site Q. The aryl C contents of the lower-size fractions are lower and the *O*-alkyl C contents and the aliphaticity (alkyl C:*O*-alkyl ratio) are clearly higher for sites P and Q than for site G. These results strongly suggest that stimulation of HA biodegradation might be achievable by continuous input of new plant litter during reforestation, even for lower-size HA polyaromatic structures, despite the fact that lower-size HAs biodegrade more slowly than higher-size HAs.

Key words: black humic acids; ^{13}C NMR spectroscopy; natural reforestation; stable isotope ratio; polyaromatic structures; radiocarbon concentration; biodegradation.

55 **1. Introduction**

56

57 Japan is a typical volcanic country, where volcanic ash soil formed from deposits of
58 volcanic material such as ash is widely distributed (Shindo et al., 2004). Many such
59 soils have very thick and dark A horizons with significant amounts of black humic acids
60 (HAs) that are major components of the humic material (Kumada, 1987; Shindo and
61 Honma, 2001). Black HAs are often characterized by extremely high aromatic and
62 stable structures (turbostratic structure; Yanagi et al., 2002, 2003), such as black carbon
63 (Kumada, 1987; Shindo et al., 1986; Shindo and Honma, 2001). The mechanisms of
64 their formation and accumulation have been discussed extensively (Hiradate et al.,
65 2004).

66 Golchin et al. (1997) reported an interesting phenomenon that occurs in typical
67 Japanese volcanic ash soil. During ca. 100 years of natural reforestation from pampas
68 grassland to deciduous broad-leaved forest via pine forest, dark A horizons were
69 decolorized. In addition, ^{13}C cross-polarization/magic-angle-spinning nuclear magnetic
70 resonance (CPMAS NMR) spectroscopy analyses of bulk soil and HAs show that the
71 aromatic C peak area decreases while the alkyl C peak area increases. We also
72 performed quantitative analysis and characterization of humic fractions using
73 liquid-state ^{13}C NMR spectroscopy at the same study site as that used by Golchin et al.
74 (1997). We found that the change in quantity and quality of soil organic matter (SOM)
75 that occurs with natural reforestation is caused specifically by the transformation of HA
76 fractions (Iimura et al., 2010). However, the detailed physicochemical properties and
77 isotopic ratios of HAs in such situations and the causes of transformation have not yet

78 been well studied.

79 HAs are heterogeneous mixtures of natural organic macromolecules. Thus, to gain
80 further insight into the chemical characteristics of soil HAs, fractionation techniques
81 such as size-exclusion chromatography (SEC) are necessary (Piccolo et al., 2002; Kuráň
82 et al., 2008). Recent studies show that high-performance SEC (HPSEC) techniques such
83 as preparative HPSEC (prep HPSEC) enable faster- and finer-size fractionation of soil
84 HAs with high reproducibility (Asakawa et al., 2011). Prep HPSEC is also reportedly
85 advantageous for HA characterization by spectroscopic methods such as ^{13}C NMR
86 spectroscopy (Conte et al., 2006).

87 The isotopic ratio of C ($\delta^{13}C$ value) in soil HAs is stable, and so is useful for
88 studying HA plant origins and estimating the rates at which natural succession from
89 grassland to forest occurs, with a resulting shift in photosynthetic strategy as the
90 dominant plant species changes from C4 to C3 (Balesdent et al., 1987; Vitorello et al.,
91 1989; López-Ulloa et al., 2005). The $\delta^{13}C$ value for atmospheric CO_2 is around −7‰;
92 the value for plant organic carbon depends on the CO_2 fixation system, with the average
93 values for carbon derived from C4 and C3 plants reported as −13‰ and −27‰,
94 respectively (Yoneyama et al., 2001). The natural radioisotope ^{14}C is useful for studying
95 HA dynamics in terrestrial environments. Radiocarbon concentration ($\Delta^{14}C$) is known
96 to directly reflect the modern C concentration in HAs (Nagao et al., 2004), making it
97 possible to consider the presence of the initial recalcitrant C in black HAs.

98 In this study, we investigated the chemical characteristics (^{13}C NMR spectroscopy),
99 degree of darkness (A_{600}/C values), and isotopic ratios ($\delta^{13}C$, $\delta^{15}N$, and $\Delta^{14}C$ values) of
100 size-separated HA fractions obtained by the prep HPSEC technique; this investigation

was conducted on samples from Japanese volcanic ash soil retrieved from the same ecological succession series—from grassland to deciduous broad-leaved forest via pine forest—which occurred over the last ca. 100 years; the investigation focused on the variation in black HA polyaromatic structures during long-term natural reforestation of Japanese pampas grassland.

2. Material and methods

2.1. Study sites and samples

The study area is situated in the campus of the Sugadaira Montane Research Center of Tsukuba University (SMRC), Nagano Prefecture, Japan. The study area is 1315 m above sea level at N 36°31′25″, E 138°20′50″. The mean annual precipitation is 1226 mm, and the mean annual temperature is 6.5 °C. Three sites within the study area were selected: sites G, P, and Q, all of which were managed as grassland for several hundred years by burning. Maintenance at site G, as of the time of this study, is performed by mowing; maintenance at sites P and Q was discontinued in the eastern area of the grassland ca. 30 and 100 years ago, respectively. Thus, the three sites collectively represent a progression in ecological succession from grassland (site G) to coniferous forest (site P) to broad-leaved forest (site Q). The dominant vegetation cover is *Miscanthus sinensis* (C4 plant) at site G, *Pinus densiflora* (C3 plant) with an understory of *Sasa* spp. (C3 plant) at site P, and *Quercus crispula* (C3 plant) with an understory of *Sasa* spp. at site Q. A few C3 plant species (*Pteridium aquilinum,* etc.) are also present

124 at site G as the minor vegetation cover. Detailed soil profiles, site sketches, aerial
125 photographs, and natural-succession histories for each site from 1950 to the present
126 were previously reported (Iimura et al., 2010).

127 Soil samples at each site were collected from the surface mineral horizon (0–20 cm)
128 after researching on soil profiles. Soil sampling points were determined after
129 preliminary research by soil auger at various points. Table 1 lists several soil
130 characteristics for each site. HA samples were the same as those purified by Iimura et al.
131 (2010).

132

133 *2.2. Mp, Mw, and polydispersity*

134

135 Prep HPSEC was performed according to the methods of Asakawa et al. (2011). For
136 estimates of molecular weight distribution, aliquots of solutions of size-separated HA
137 fractions were diluted (50×) with eluent and analyzed by analytical HPSEC (Asakawa et
138 al., 2008). Molecular weight at peak maximum (Mp), weight-averaged molecular
139 weight (Mw), and polydispersity were calculated with Waters Millenium 32
140 Chromatography Manager version 3.06 software. For other analyses, evaporated
141 solutions of each size fraction were acidified to pH 1.0 with 6 M HCl, dialyzed in
142 deionized water (Spectra/Por CE membrane, M_W cutoff 500 Da, Spectrum, Houston,
143 TEX, USA), and freeze dried.

144

145 *2.3. Degree of darkness*

146

147 The degree of darkness (A_{600}/C values) of the size-separated HA fractions was
148 determined according to the methods of Ikeya and Watanabe (2003), where A_{600} is the
149 absorbance at 600 nm and C is the organic C concentration. A_{600} was measured on a
150 UV–vis spectrophotometer (Jusco V-530). C was measured on a TOC analyzer
151 (Shimadzu TOC-V), with samples prepared as follows: HAs were dissolved in 0.1M
152 NaOH for determine the absorbance at 600 nm, the solution was adjusted to about pH 4
153 by dilution (5×) with 0.066 M kH_2PO_4 and dissolved CO_2 was removed by bubbling
154 with N_2 for determine the organic C concentration.
155
156 *2.4. Elemental composition and $\delta^{13}C$, $\delta^{15}N$, $\Delta^{14}C$ values*
157
158 Elemental analysis of the size-separated HA fractions was performed on a CHNS/O
159 analyzer (PerkinElmer 2400II) using 2 mg of dry sample per measurement. Ash content
160 was determined after combustion of 10 mg of dry sample at 550 °C in a muffle furnace
161 for 4 h.
162 Isotopic analysis on samples were accomplished with an elemental analyzer coupled
163 with an IsoPrime EA stable isotope ratio mass spectrometer (GV Instruments, UK).
164 $\delta^{13}C$ and $\delta^{15}N$ values were calculated as follows:
165
166 $\delta^{13}C$ or $\delta^{15}N = [R_{sample}/R_{standard} - 1] \times 1000$,
167
168 where R is the ^{13}C:^{12}C or ^{15}N:^{14}N ratio in the sample and the standard. Reference
169 material USGS 40 (L-glutamic acid) with $\delta^{13}C = -26.4$ ‰ and $\delta^{15}N = -4.5$ ‰ was used

as a calibrated standard, and results were reported relative to Peedee belemnite (PDB) and air. The standard deviation of a measurement based on multiple analyses of the standard was generally ≤0.1‰. Each sample was analyzed in three replicates. If the standard deviation was >0.2‰, the measurement was repeated until the standard deviation for all measurements fell to ≤0.2‰. The contribution ratios of C4-plant-derived and C3-plant-derived carbon on the carbon of the sample (CR_{C4} and CR_{C3}) were calculated as follows:

$$\delta^{13}C = \delta C_4 \times CR_{C4} + \delta C_3 \times (1 - CR_{C4}),$$

$$CR_{C3} = 100 - CR_{C4},$$

where δC_4 and δC_3 are the $\delta^{13}C$ values of C4- and C3-plant-derived carbon, respectively (Hiradate et al., 2004). In the present study, the δC_4 and δC_3 values were set to −13‰ and −27‰, respectively (Yoneyama et al., 2001). The C content derived from C3 and C4 plants was then calculated for the size-separated HA fractions from the C content of each HA fraction and CR_{C3} and CR_{C4}.

The ^{14}C contents of selected HA fractions were determined at the AMS facility (NIES-TERRA) of the National Institute for Environmental Study (Uchida et al., 2004). Sample graphitization was carried out according to the method of Uchida et al. (2005, 2008) as follows: Homogenized bulk sediment samples were combusted in sealed quartz tubes (with CuO), and the resulting CO_2 was purified and graphitized by reduction with H_2 in the presence of Fe powder as a catalyst.

193 *2.5. Liquid-state ^{13}C NMR*

194

195 Liquid-state ^{13}C NMR spectra were recorded with an NMR spectrometer (Avance
196 500, Bruker GmbH, Karlsruhe, Germany) using sample tubes with 5 mm in diameter.
197 Samples (ca. 30–50 mg) were dissolved in 0.4 ml of 0.5 mol l^{-1} NaOD in D_2O.
198 Chemical shifts were referenced to sodium 3-trimethylsilylpropionate-2,2,3,3-D_4 (TSP;
199 Euriso-top, Saint Aubin, France). To obtain quantitative conditions for integration of the
200 ^{13}C NMR spectra, ^{13}C signals were proton-decoupled using the following inverse-gated
201 decoupling technique parameters: spectrometer frequency = 125.76 MHz, pulse width =
202 45°, acquisition time = 0.839 s, and total repetition time = 2.5 s. To improve the
203 signal/noise ratio, line broadening of 50 Hz was used. Scans from 10,000 to 20,000
204 were accumulated. Resonance areas were calculated by electronic integration. Spectral
205 peaks were assigned according to the reports of Preston and Blackwell (1985), Schnitzer
206 and Preston (1986), Thorn et al. (1989), and Ricca and Severini (1993). To obtain
207 quantitative information, the spectra were divided into the following six regions
208 (Fujitake and Kawahigashi, 1999): alkyl C, 5–45 ppm; *O*-alkyl C, 45–110 ppm; aryl C,
209 110–145 ppm; *O*-aryl C, 145–165 ppm; carboxylic C, 165–190 ppm; and carbonyl C,
210 190–220 ppm. Aromaticity, as proposed by Watanabe and Fujitake (2008), was
211 expressed as the ratio of aryl C and *O*-aryl C to the total of alkyl C, *O*-alkyl C, aryl C,
212 and *O*-aryl C. Aliphaticity, as proposed by Golchin et al. (1995), was expressed as the
213 ratio of alkyl C to *O*-alky l C.

214

215 **3. Results and discussion**

216

217 *3.1. Dynamics of isotopic ratios and their relationship with degree of darkness*

218

219 For all sites, the $\delta^{13}C$ value for each size-separated HA fraction increases with $\delta^{15}N$
220 value, although the gradient of the trend differs according to molecular size (Fig. 1).
221 The $\delta^{13}C$: $\delta^{15}N$ ratios at each site are generally as follows: data for site G Fr. 1–4, site P
222 Fr. 1–5, and site Q Fr. 1–6 fall along the 1:3 line and data for site G Fr. 5–10, site P Fr.
223 6–10, and site Q Fr. 7–10 (except for Fr. 8) fall along the 1:1 line. Greater ^{13}C and ^{15}N
224 enrichment in SOM often reflects the degree of biodegradation and humification
225 (Marin-Spiotta et al., 2009). In addition, Connin et al. (2001) reported that the $\delta^{15}N$
226 value clearly increases relative to the $\delta^{13}C$ value with microbial degradation of litter that
227 is easily decomposed by microorganisms. Therefore, our $\delta^{13}C$: $\delta^{15}N$ ratio data suggest
228 that black HAs consist of two major components. Furthermore, within the same black
229 HA, components that generally fall along the 1:1 line may be more resistant to
230 microbial attack than those that fall along the 1:3 line.

231 The values of maximum peak molecular weight (Mp) and weight-averaged
232 molecular weight (Mw) for size-separated HA fractions clearly decrease with Fr.
233 number for all sites (Table 2). We therefore categorized Fr. 1–4 of site G, Fr. 1–5 of site
234 P, and Fr. 1–6 of site Q as higher-molecular-size fractions and Fr. 5–10 of site G, Fr.
235 6–10 of site P, and Fr. 7–10 of site Q as lower-molecular-size fractions based on the
236 $\delta^{13}C$: $\delta^{15}N$ ratio, Mp, and Mw within the same HA.

237 Table 3 shows the carbon content C derived from C3 and C4 plants for
238 size-separated HA fractions from each site. Fig. 2 also shows their relationship with the

239 degree of darkness (A_{600}/C values) for size-separated HA fractions from each site. The
240 estimated carbon content C derived from C4 plants in the lower-size fraction ranges are
241 as follows: site G 2.3–3.4 C g kg^{-1}, site P 2.2–2.6 C g kg^{-1}, and site Q 0.8–0.9 C g kg^{-1}
242 (Table 3). These values for the lower-size fractions of each HA correlate positively with
243 A_{600}/C values: r = 0.73 at site G, r = 0.77 at site P, and r = 0.91 at site Q (Fig. 2). In
244 contrast, the correlation coefficients of estimated carbon content C derived from C4
245 plants and A_{600}/C values in the higher-size fractions were much lower than those in the
246 lower-size fractions: r = 0.03 at site G, r = 0.01 at site P, and r = −0.75 at site Q (Fig.2).
247 A_{600}/C values for HAs are known to commonly correlate positively with aromatic C
248 content and C-layer plane size (Watanabe et al., 2005; Ikeya et al., 2011). Yamanoi
249 (1996) emphasized the importance of microparticles of charred pampas grassland (C4
250 plant) in the formation and accumulation of black HAs in Japanese volcanic ash soils.
251 Hiradate et al. (2004) also showed that the proportion of aromatic C in HAs correlates
252 significantly with the amount of C derived from the C4 plant of HAs from Japanese
253 volcanic ash soils. Our results therefore strongly suggest that the lower-size components
254 of black HAs have more stable charred C4-plant-derived C than do the higher-size
255 components within the same HAs. Furthermore, the mean values of carbon content C
256 derived from C4 plants of the lower-size components (site G 2.9 C g kg^{-1}, site P 2.4 C g
257 kg^{-1}, site Q 0.8 C g kg^{-1}) decrease much more during natural reforestation than do the
258 estimated C derived from C3 plants (site G 2.9 C g kg^{-1}, site P 2.2 C g kg^{-1}, site Q 2.1 C
259 g kg^{-1}), particularly from site P to site Q (Table 3).
260 In the long term (ca. 100 years), invasion of woody vegetation (C3 plants) into
261 grassland is generally thought to lead to an increase in the amount of litter input

(Jackson et al., 2002). This continuous addition of litter, particularly in deciduous broad-leaved forests, probably compensates for the loss of C4-plant-derived C. In our study, the A_{600}/C values for the different size fractions in each HA do not correlate well positively with C3-plant-derived C, and C content appears to not change significantly during reforestation, in contrast to the case for C4-plant-derived C (Fig. 2 and Table 3). The $\delta^{13}C$ values across size fractions are also lower for site Q (from −23.2‰ to −22.2‰) than for site G (from −20.9‰ to −19.1‰) and site P (from −20.2‰ to −19.1‰) (Table 3), suggesting higher incorporation of products derived from newer C3 forests across all size fractions during long-term reforestation.

The variation in $\Delta^{14}C$ value with molecular size shows a similar trend for all HAs: first decreasing as molecular size increases from small to medium, then increasing as molecular size increases from medium to large (Table 3). Based on our data for A_{600}/C, $\delta^{13}C$, and $\delta^{15}N$ values, we suggest that the more stable lower-size components in black HAs may undergo different humification (stabilization) processes than do the less stable higher-size components. As evidence, lower-size components showed that with increasing molecular size, A_{600}/C and $\delta^{15}N$ values increase while the $\Delta^{14}C$ value decreases (Figs. 1 and 2, Table 3). In addition, the $\Delta^{14}C$ values of size fractions in both forest sites (sites P and Q) showed clearly higher values than those of site G (Table 3). $\Delta^{14}C$ values for atmospheric CO_2 measured prior to atmospheric nuclear testing in the 1950s were ≤0‰; therefore, the measured $\Delta^{14}C$ values directly reflect the presence of modern C introduced by nuclear weapon testing during the 1950s and 1960s (Nagao et al., 2004). Thus, our results show that the amount of modern C in HAs increases with reforestation even in the lower-size fractions, particularly in the earlier stages of

285 reforestation (from site G to P) (Table 3). The reasons for this are discussed along with
286 ^{13}C NMR spectroscopy data in the next section.
287
288 *3.2. Dynamics of black HAs during natural reforestation*
289
290 ^{13}C NMR spectra and the C content of the functional groups of the size-separated
291 HA fractions are shown in Fig. 3 and listed in Table 4. All samples show essentially the
292 same peaks in the general chemical-shift regions, although peak magnitude varies. For
293 all HAs, molecular size correlates negatively with aryl C and positively with *O*-alkyl C
294 and alkyl C. For site G, total aryl C content is high (except for the largest-size fraction)
295 and *O*-alkyl C and alkyl C contents are relatively low (Table 4). In contrast, for sites P
296 and Q, total aryl C content decreases with increasing molecular size, whereas *O*-alkyl C
297 and alkyl C contents are more similar to those at site G (Table 4). These results strongly
298 support our abovementioned suggestion that for black HAs, lower-size components
299 undergo a different humification process than do higher-size components, and have
300 more polyaromatic structures derived from charred C4-plant materials; these moieties
301 may disappear during long-term natural reforestation.
302 Continuous input of fresh plant litter is well known to result in accumulation of
303 material that is highly resistant to biodegradation, such as resins, waxes, and other lipids
304 (Ziegler and Zech, 1989; Kogel-Knabner et al., 1992; Zech et al., 1992). In addition, the
305 trend of decreasing *O*-alkyl C and increasing alkyl C content (aliphaticity) with
306 decomposition has been reported for various soil types (Baldock et al., 1992; Golchin et
307 al., 1995). Furthermore, Willmann and Fakoussa (1997) demonstrated that HAs show

308 increased aliphatic C (*O*-alkyl and alkyl C), together with decreased aryl C, after
309 incubation of the white rot fungal strain. Thus, the higher aliphatic chemical
310 characteristics of each size fraction in the present study (Table 4, Fig. 3) may be caused
311 by selective biodegradation of some HAs moieties and selective incorporation of
312 products derived from microbial synthesis and/or plant litter.

313 Our $\delta^{13}C$ data do not fully explain the higher incorporation of products derived from
314 newer C3 plants (forests and floor plants) across all size fractions during reforestation
315 from site G to P (Table 3). Alfredsson et al. (1998) reported that the decrease in soil C
316 with reforestation on temperate grassland may be attributed to changes in soil
317 macroflora and microflora associated with the root/rhizosphere systems in forest as
318 opposed to grassland. For example, ectomycorrhizal fungi associated with tree roots
319 have been found to increase the mineralization of organic matter in soil via production
320 of extracellular hydrolase enzymes (Marschner and Dell, 1994; George and Marschner,
321 1996). Overall, our measured C:N ratios are lower (Table 3) and aliphaticity is higher
322 (Table 4) for size fractions at site P than for those at site G, suggesting that microbial
323 activity is higher at site P than at site G.

324 This change in the microbial activity may reflect the difference in the chemical
325 properties and $\Delta^{14}C$ values for the size fractions at sites G and P. Kleber and Johnson
326 (2010) emphasized that the concentration of ^{14}C in an organic molecule is not at all
327 related to its chemical stability. They also stated that a decomposer organism is
328 indifferent to the ^{14}C content of an organic molecule. In our case, a clear difference in
329 the $\Delta^{14}C$ values of lower-size and higher-size fractions is not evident for all sites (Table
330 3). This agrees well with the report of Kleber and Johnson (2010). However, when the

vegetation cover changed drastically, the $\Delta^{14}C$ values as well as the chemical properties of size fractions may be varied. For sites G and P, our data on the variation of C4-plant-derived C as well as on the values of A_{600}/C values, $\delta^{13}C$, and $\delta^{15}N$ suggest that the higher *O*-alkyl and alkyl C of size fractions from site P as compared with those from site G may be caused mainly by selective biodegradation of HA moieties (old C) except for the polyaromatic structures derived from charred C4-plant materials. For site Q, the situation may differ; our data suggest a higher incorporation of products derived from newer C3 plants (forest and floor plants) across all size fractions during reforestation from site P to Q (Fig. 2 and Table 3). Hamer et al. (2004) reported that mineralization of black carbon is stimulated by the addition of glucose. Indeed, the *O*-alkyl C content (e.g., carbohydrate C) and aliphaticity is higher for size fractions from site Q than for those from site G, even in lower-size fractions, as shown for site P (Table 4). In addition, A_{600}/C values and C4-plant-derived C content for lower-size fractions are clearly lower for site Q than for sites G and P (Fig. 2). Therefore, we speculate that stimulating black HA biodegradation, even if the polyaromatic structures are presumably derived from charred materials, may be achievable by continuous input of new litter (deciduous leaves) during long-term reforestation, despite the fact that biodegradation is slower for lower-size than for higher-size components.

4. Conclusions

Our study strongly suggests that black HAs in Japanese volcanic ash soil consist of two major types of components: one with a relatively lower molecular size and a

354 polyaromatic character (presumably derived from charred materials) and other with a
355 relatively higher molecular size and an aliphatic character. Lower-size components
356 exhibit slower rates of variation in their stable isotope ratios than do higher-size
357 components, strongly suggesting that stimulating the biodegradation of black HAs, even
358 of its lower-size components, can be achieved by continuous input of new litter such as
359 carbohydrate C moieties during long-term natural reforestation of Japanese pampas
360 grassland.
361
362 **Acknowledgments**
363
364 The study was supported by a Grant-in-Aid for Scientific Research (B-16380049,
365 2004-2006) from the Japan Society for the Promotion of Science and Environment
366 Research and Technology Development Fund (A-1003) of the Ministry of the
367 Environment, Japan. We are also grateful to T. Iida and T. Kobayashi for the operation
368 of AMS (NIES-TERRA).

References

Alfredsson, H., Condron, L.M., Clarholm, M., Davis, M.R., 1998. Changes in soil acidity and organic matter following the establishment of conifers on former grassland in New Zealand. Forest Ecology and Management 112, 245−252.

Asakawa, D., Kiyota, T., Yanagi, Y., Fujitake, N., 2008. Development and validation of method of high-performance size-exclusion chromatography (HPSEC) for various soil humic acids. Analytical Sciences 24, 607–613.

Asakawa, D., Iimura, Y., Kiyota, T., Yanagi, Y., Fujitake, N., 2011. Molecular size fractionation of soil humic acids using preparative high performance size-exclusion chromatography. Journal of Chromatography A 1218, 6448–6453.

Baldock, J.A., Oades, J., Waters, A.G., Peng, X., Vassallo, A.M., Wilson, M.A., 1992. Aspects of the chemical structure of soil organic materials as revealed by solid-state ^{13}C NMR spectroscopy. Biogeochemistry 16, 1–42.

Balesdent, J.M., Mariotti, A., Guillet, B., 1987. Natural ^{13}C abundance as a tracer for studies of soil organic matter dynamics. Soil Biology and Biochemistry 19, 25–30.

Connin, S.L., Feng, X., Virginia, R.A., 2001. Isotopic discrimination during long-term decomposition in an arid land ecosystem. Soil Biology and Biochemistry 33, 41–51.

Conte, P., Spaccini, R., Piccolo, A., 2006. Advanced CPMAS-^{13}C NMR techniques for molecular characterization of size-separated fractions from a soil humic acid. Analytical and Bioanalytical Chemistry 286, 382–390.

Fujitake, N., Kawahigashi, M., 1999. ^{13}C NMR spectra and elemental composition of fractions with different particle size from an andosol humic acid. Soil Science and

392 Plant Nutrition 45, 359–366.
393 George, E., Marschner, H., 1996. Nutrient and water uptake by roots of forest trees.
394 Journal of Plant Nutrition and Soil Science 159, 11−21.
395 Golchin, A., Clark, P., Baldock, J.A., Higashi, T., Skjemstad, J.O., Oades, J.M., 1997.
396 The effect of vegetation and burning on the chemical composition of soil organic
397 matter in a volcanic ash soil as shown by ^{13}C NMR spectroscopy. I. Whole soil and
398 humic acid fraction. Geoderma 76, 155–174.
399 Golchin, A., Oades, J.M., Skjemstad, J.O., Clarke, P., 1995. Structural and dynamic
400 properties of soil organic matter as reflected by ^{13}C natural abundance, pyrolysis
401 mass spectrometry and solid-state ^{13}C NMR spectroscopy in density fractions of an
402 Oxisol under forest and pasture. Australian Journal of Soil Research 33, 59–76.
403 Hamer, U., Marschner, B., Brodowski, S., Amelung, W., 2004. Interactive priming of
404 black carbon and glucose mineralisation. Organic Geochemistry 35, 823–830.
405 Hiradate, S., Nakadai, T., Shindo, H., Yoneyama, T., 2004. Carbon source of humic
406 substances in some Japanese volcanic ash soils determined by carbon stable isotopic
407 ratio, $\delta^{13}C$. Geoderma 119, 133–141.
408 Iimura, Y., Fujimoto, M., Hirota, M., Tamura, K., Higashi, T., Yonebayashi, K.,
409 Fujitake, N., 2010. Effects of ecological succession on surface mineral horizons in
410 Japanese volcanic ash soil. Geoderma 159, 122–130.
411 Ikeya, K., Hikage, T., Arai, S., Watanabe, A., 2011. Size distribution of condensed
412 aromatic rings in various soil humic acids. Organic Geochemistry 42, 55–61.
413 Ikeya, K., Watanabe, A., 2003. Direct expression of an index for the degree of
414 humification of humic acids using organic carbon concentration. Soil Science and

Plant Nutrition 49, 47–53.

Jackson, R.B., Banner, J.L., Jobbagy, E.G., Pockman, W.T., Wall, D.H., 2002. Ecosystem carbon loss with woody plant invasion of grasslands. Nature 418, 623–626.

Kleber, M., Johnson, M.G., 2010. Advances in understanding the molecular structure of soil organic matter: Implications for interactions in the environment. Advances in Agronomy 106, pp. 105.

Kögel-Knabner, I., Leeuw, J.W., Hatcher, P.G., 1992. Nature and distribution of alkyl carbon in forest soil profiles: implication for the origin and humification of aliphatic biomacromolecules. The Science of the Total Environment 117/118, 175–185.

Kumada, K., 1987. Chemistry of Soil Organic Matter. Japan Scientific Societies Press, Elsevier, Amsterdam, pp. 181–204.

Kuráň, P., Janoš, P., Madronová, L., Novák, J., Kozler, J., 2008. Determination of OH groups in humic acids using methylation with dimethylsulfate. Talanta 76, 960–963.

López-Ulloa, M., Veldkamp, E., Koning, H.G.J., 2005. Soil carbon stabilization in converted tropical pastures and forests depends on soil type. Soil Science Society of American Journal 69, 1110–1117.

Marin-Spiotta, E., Silver, W., Swanston, C.W., Ostertag, R., 2009. Soil organic matter dynamics during 80 years of reforestation of tropical pastures. Global Change Biology 15, 1584–1597.

Marschner, H., Dell, B., 1994. Nutrient uptake in mycorrhizal symbiosis. Plant and Soil 159, 89−102.

Nagao, S., Aramaki, T., Fujitake, N., Matsunaga, T., Tkachenko, Y., 2004 Radiocarbon

438 of dissolved humic substances in river waters from the Chernobyl area. Nuclear
439 Instruments and Methods in Physical Research B 223–224, 848–853.
440 Piccolo, A., Conte, P., Trivellone, E., Van Lagen, B., Buuman, P., 2002 Reduced
441 heterogeneity of a lignite humic acid by Preparative HPSEC following interaction
442 with an organic acid. Characterization of size-separates by Pyr-GC-MS and
443 ^{1}H-NMR spectroscopy. Environmental Science and Technology 36, 76–84.
444 Preston, C.M., Blackwell, B.A., 1985. Carbon-^{13}C nuclear magnetic resonance for a
445 humic and a fulvic acid: signal-to-noise optimization, quantitation, and spin-echo
446 techniques. Soil Science 139, 88–96.
447 Ricca, G., Severini, F., 1993. Structural investigations of humic substances by IR-FT,
448 ^{13}C-NMR spectroscopy and comparison with a maleic oligomer of known structure.
449 Geoderma 58, 233–244.
450 Schnitzer, M., Preston, C.M., 1986. Analysis of humic acids by solution and solid-state
451 ^{13}C nuclear magnetic resonance. Soil Science Society of American Journal 50,
452 326–331.
453 Shindo, H., Honma, H., 2001. Significance of burning vegetation in the formation of
454 black humic acids in Japanese volcanic ash soils. In: Ghabbour. E.A., Davies, G.
455 (Eds.), Humic Substances, Structures, Models and Function. Royal Society of
456 Chemistry, Cambridge, UK, pp. 293–306.
457 Shindo, H., Honna, T., Yamamoto, S., Honma, H., 2004. Contribution of charred plant
458 fragments to soil organic carbon in Japanese volcanic ash soils containing black
459 humic acids. Organic Geochemistry 35, 235–241.
460 Shindo, H., Matsui, Y., Higashi, T., 1986. A possible source of humic acids in volcanic

461 ash soils in Japan-charred residue of *Miscanthus sinensis*. Soil science 141, 84–87.
462 Thorn, K.A., Folan, D.W., MacCarthy, P., 1989. Characterization of the International
463 Humic Substances Society: standard and reference fulvic and humic acids by
464 solution state carbon-13 (^{13}C) and hydrogen-1 (^{1}H) nuclear magnetic resonance
465 spectrometry. In: Water Resource Investigations Report 89−4196, US Geological
466 Survey, Denver, US, pp. 1–93.
467 Uchida, M., Shibata, Y., Yoneda, M., Kobayashi, T., Morita, M., 2004. Technical
468 progress in AMS microscale radiocarbon analysis. Nuclear Instruments and
469 Methods in Physics Research B 233–234, 313–317.
470 Uchida, M., Shibata, Y., Ohkushi, K., Yoneda, M., Kawamura, K., Morita, M., 2005.
471 Age discrepancy between molecular biomarkers and calcareous foraminifera
472 isolated from the same horizons of Northwest Pacific sediments. Chemical Geology
473 218, 73–89.
474 Uchida, M., Ohkushi, K., Kimoto, K., Inagaki, F., Ishimura, T., Tsunogai, U., TuZino,
475 T., Shibata, Y., 2008. Radiocarbon-based carbon source quantification of anomalous
476 isotopic foraminifera in last glacial sediments in the western North Pacific.
477 Geochemistry Geophysics Geosystems 9, doi: 10.1029/2006GC001558.
478 Vitorello, V.A., Cerri, C.C., Andreaux, F., Feller, C., Victoria, R.L., 1989. Organic
479 matter and natural carbon-13 distribution in forested and cultivated Oxisols. Soil
480 Science Society of American Journal 53, 773–778.
481 Watanabe, A., Fujitake, N., 2008. Comparability of composition of carbon functional
482 groups in humic acids between inverse-grated decoupling and cross
483 polarization/magic angle spinning ^{13}C nuclear magnetic resonance techniques.

484 Analytica Chimica Acta 618, 110–115.
485 Watanabe, A., Mcphail, D., Maie, N., Kawasaki, S., Anderson, H., Cheshire, M., 2005.
486 Electron spin resonance characteristics of humic acids from a wide range of soil
487 types. Organic Geochemistry 36, 981–990.
488 Willmann, G., Fakoussa, R.M., 1997. Biological bleaching of water-soluble coal
489 macromolecules by a basidiomycete strain. Applied Microbiology and
490 Biotechnology 47, 95–101.
491 Yamanoi, T., 1996. Geological investigation of the origin of the black soil, distributed
492 in Japan. Journal of the Geological Society of Japan 102, 526–544 (in Japanese with
493 English summary).
494 Yanagi, Y., Hamaguchi, S., Tamaki, H., Suzuki, T., Otsuka, H., Fujitake, N., 2003.
495 Relation of chemical properties of soil humic acids to decolorization by white rot
496 fungus−*Coriolus consors*. Soil Science and Plant Nutrition 49, 201–206.
497 Yanagi, Y., Tamaki, H., Otsuka, H., Fujitake, N., 2002. Comparison of decolorization
498 by microorganisms of humic ands with different ^{13}C NMR properties. Soil Biology
499 and Biochemistry 34, 729–731.
500 Yoneyama, T., Nakanishi, Y., Morita, A., Liyanage, B.C., 2001. $\delta^{13}C$ values of organic
501 carbon in cropland and forest soils in Japan. Soil Science and Plant Nutrition 47,
502 17–26.
503 Zech, W., Ziegler, F., Kögel-Knabner, I., Haumaier, L., 1992. Humic substances
504 distribution and transgormation in forest soils. The Science of the Total
505 Environment 117/118, 155–174.
506 Ziegler, F., Zech, W., 1989. Distribution pattern of total lipids and lipid fractions in

forest humus. Zeitschrift für Pflanzenernährung und Bodenkunde 152, 287–290.

508 **Figure captions**

509

510 **Fig. 1.** Relationship between $\delta^{13}C$ and $\delta^{15}N$ values for size-separated HAs fractions
511 taken from each study site. The numbers indicate the fraction number.

512

513 **Fig. 2.** Carbon derived from C3- and C4-plant content and degree of darkness (A_{600}/C
514 values) for size-separated HAs fractions taken from each study site.

515

516 **Fig. 3.** ^{13}C NMR spectra of size-separated HAs fractions taken from each study site.

517 **Table 1**

518 Selected characteristics of soils used.

Sample	Depth (cm)	pH[a] (H_2O)	pH[a] (NaF)	T-C[a] (g kg^{-1} soil)	T-N[a] (g kg^{-1} soil)	Bulk density (g cm^{-1})	HA fraction[a] (gC kg^{-1} soil)
Site G	0-20	6.0	10.7	134	12.1	0.42	60.4
Site P	0-20	5.2	10.8	122	7.2	0.45	47.4
Site Q	0-20	5.3	11.3	88	4.6	0.51	30.2

519 [a] These data are from Iimura et al. (2010).

520 **Table 2**

521 Maximum peak molecular weight (Mp), weight-averaged molecular weight (Mw), and
522 polydispersity (Mw/Mn) of whole and size fractions of HAs estimated from calibration
523 curve of sodium polystyrene sulfonate (PSSNa).

HAs	Apparent molecular weight (kDa)[a]		Polydispersity[b]
	Mw	Mp	(Mw/Mn)
Site G			
Whole	5.35	2.79	3.10
Fr.1	28.9	20.4	15.3
Fr.2	14.3	13.1	3.70
Fr.3	12.4	11.0	2.00
Fr.4	9.11	8.41	2.38
Fr.5	7.74	7.18	2.01
Fr.6	6.35	5.80	1.74
Fr.7	5.49	4.87	1.66
Fr.8	4.61	3.85	1.59
Fr.9	3.73	3.09	1.56
Fr.10	2.39	2.03	1.61
Site P			
Whole	8.00	3.32	9.50
Fr.1	88.4	58.1	22.5
Fr.2	36.8	26.7	16.4
Fr.3	22.1	17.5	4.04
Fr.4	18.0	14.4	3.33
Fr.5	14.8	11.9	2.27
Fr.6	11.7	9.66	2.64
Fr.7	9.76	8.03	2.43
Fr.8	8.46	6.82	2.24
Fr.9	6.23	5.07	2.43
Fr.10	3.42	2.66	2.42
Site Q			
Whole	12.9	3.61	5.55
Fr.1	58.8	34.6	4.88
Fr.2	20.4	17.3	1.96
Fr.3	13.2	11.8	2.68
Fr.4	9.72	8.85	3.14
Fr.5	7.99	7.15	2.75
Fr.6	6.74	6.00	2.42
Fr.7	5.70	4.91	2.22
Fr.8	4.65	4.02	2.05
Fr.9	3.76	3.09	1.87
Fr.10	2.38	1.98	1.89

524 [a] Except for site P, data are from Asakawa et al. (2011), which are matching of site G

525 and Q to SGG and SGM HA, respectively.

526 [b] Polydispersity is the ratio of the weight-averaged (Mw) to number-averaged

527 molecular weight (Mn).

528 **Table 3**

529 C and N contents, isotopic ratios ($\delta^{13}C$, $\delta^{15}N$ and $\Delta^{14}C$ values), and C3- and

530 C4-plant-derived C contents of whole and size-separated HAs fractions.

Sample	C ($g\ kg^{-1}$)	N ($g\ kg^{-1}$)	C/N	$\delta^{13}C$ (‰)	C3-C[a] ($g\ kg^{-1}$)	C4-C[b] ($g\ kg^{-1}$)	$\delta^{15}N$ (‰)	$\Delta^{14}C$ (‰)
Site G								
whole	60.4	3.46	17.5	−19.6	28.4	32.0	4.41	−212
Fr.1	6.2	0.34	18.2	−19.1	2.7	3.6	5.19	−156
Fr.2	6.4	0.42	15.4	−19.1	2.8	3.6	4.50	
Fr.3	6.2	0.31	19.8	−19.4	2.8	3.3	3.89	−228
Fr.4	6.9	0.34	20.5	−19.4	3.2	3.7	3.75	
Fr.5	5.5	0.30	18.5	−19.6	2.6	2.9	4.72	−222
Fr.6	6.4	0.35	18.3	−19.6	3.0	3.4	4.50	
Fr.7	5.7	0.34	17.0	−19.7	2.7	3.0	4.39	−225
Fr.8	5.9	0.38	15.5	−19.9	2.9	3.0	4.38	
Fr.9	6.0	0.31	19.4	−20.2	3.1	2.9	4.01	−199
Fr.10	5.2	0.39	13.4	−20.9	2.9	2.3	4.00	
Site P								
whole	47.4	3.52	13.5	−19.6	22.3	25.1	4.45	24
Fr.1	4.9	0.32	15.1	−19.1	2.1	2.8	4.83	22
Fr.2	4.9	0.38	12.9	−19.2	2.2	2.8	4.95	
Fr.3	4.9	0.36	13.7	−19.3	2.2	2.7	4.66	19
Fr.4	4.9	0.35	13.9	−19.5	2.3	2.7	4.39	
Fr.5	4.5	0.33	13.6	−19.4	2.1	2.4	4.39	5
Fr.6	4.8	0.52	9.1	−19.5	2.2	2.6	4.56	
Fr.7	4.5	0.32	14.1	−19.6	2.1	2.4	4.64	
Fr.8	4.7	0.32	14.5	−19.6	2.2	2.5	4.57	
Fr.9	4.8	0.33	14.3	−19.7	2.3	2.5	4.53	27
Fr.10	4.5	0.27	16.7	−20.2	2.3	2.2	4.13	
Site Q								
whole	30.2	2.08	14.5	−22.6	20.5	9.7	5.18	−16
Fr.1	3.1	0.22	14.4	−22.2	2.0	1.1	5.72	10
Fr.2	3.1	0.23	13.6	−22.5	2.1	1.0	5.40	
Fr.3	3.1	0.22	13.6	−22.5	2.1	1.0	4.95	−15
Fr.4	3.0	0.22	13.9	−22.5	2.1	1.0	4.84	
Fr.5	3.0	0.23	12.8	−22.6	2.0	1.0	4.52	−80
Fr.6	3.0	0.24	12.5	−22.7	2.0	0.9	4.12	
Fr.7	3.0	0.20	15.2	−22.9	2.1	0.9	4.63	−35
Fr.8	3.1	0.20	15.5	−23.0	2.2	0.9	4.07	
Fr.9	3.0	0.17	17.4	−23.1	2.1	0.8	4.49	−7
Fr.10	2.9	0.16	18.6	−23.2	2.2	0.8	4.40	

531 [a] Carbon content C derived from C3-plants.

532 [b] Carbon content C derived from C4-plants.

533

534 **Table 4**

535 Composition of C functional groups, aromaticity and aliphaticity of size-separated HAs

536 estimated from ^{13}C NMR.

HAs	% of carbon species (δ, ppm)						aromaticity	aliphaticity
	carbonyl 220-190	carboxyl 190-165	*O*-aryl 165-145	aryl 145-110	*O*-alkyl 110-45	alkyl 45-5		
Site G								
Fr.1	1.8	18.4	3.0	23.6	34.6	18.5	0.33	0.54
Fr.2[a]								
Fr.3	2.0	16.6	9.0	37.8	22.8	11.8	0.57	0.52
Fr.4	3.0	19.9	7.7	43.3	15.8	10.3	0.66	0.66
Fr.5	3.4	18.5	10.0	38.5	19.6	9.91	0.62	0.50
Fr.6	1.2	17.8	8.4	33.5	25.2	13.8	0.52	0.55
Fr.7	3.8	17.0	10.4	39.6	18.3	10.9	0.63	0.60
Fr.8	2.5	15.9	6.8	44.9	17.9	11.9	0.63	0.67
Fr.9	3.6	17.9	7.5	47.7	14.0	9.36	0.70	0.67
Fr.10	0.9	15.5	7.4	45.8	18.5	12.0	0.64	0.65
Site P								
Fr.1	5.1	13.8	4.4	11.5	41.3	24.0	0.20	0.58
Fr.2	4.4	12.9	6.9	18.2	34.7	22.8	0.30	0.66
Fr.3	5.3	17.3	8.8	21.8	28.8	18.0	0.40	0.62
Fr.4	7.1	17.2	7.6	18.3	29.9	19.9	0.34	0.66
Fr.5	4.0	17.0	8.4	21.3	29.3	20.0	0.38	0.68
Fr.6	6.1	16.6	7.8	23.6	27.7	18.3	0.41	0.66
Fr.7	5.1	15.3	6.2	24.5	29.6	19.3	0.39	0.65
Fr.8	5.8	15.0	7.3	20.0	29.9	22.1	0.34	0.74
Fr.9	4.1	17.9	6.8	29.9	23.8	17.4	0.47	0.73
Fr.10	5.4	17.2	7.2	33.0	21.2	15.9	0.52	0.75
Site Q								
Fr.1	6.0	19.3	7.0	22.8	25.4	19.4	0.40	0.76
Fr.2	4.2	18.1	4.8	20.6	31.2	21.1	0.33	0.68
Fr.3	3.0	17.7	6.2	26.3	27.1	19.6	0.41	0.72
Fr.4	3.7	19.8	7.9	29.9	22.4	16.2	0.50	0.72
Fr.5	2.1	18.2	6.0	25.8	26.4	21.5	0.40	0.81
Fr.6	3.0	18.9	6.7	31.3	23.0	17.1	0.49	0.74
Fr.7	4.0	19.1	6.7	34.0	20.6	15.6	0.53	0.76
Fr.8	2.8	19.3	5.8	32.9	23.0	16.2	0.50	0.70
Fr.9	2.8	18.6	7.9	34.2	22.4	14.1	0.54	0.63
Fr.10	3.5	20.7	7.6	35.8	18.9	13.6	0.57	0.72

537 [a] Not determined.

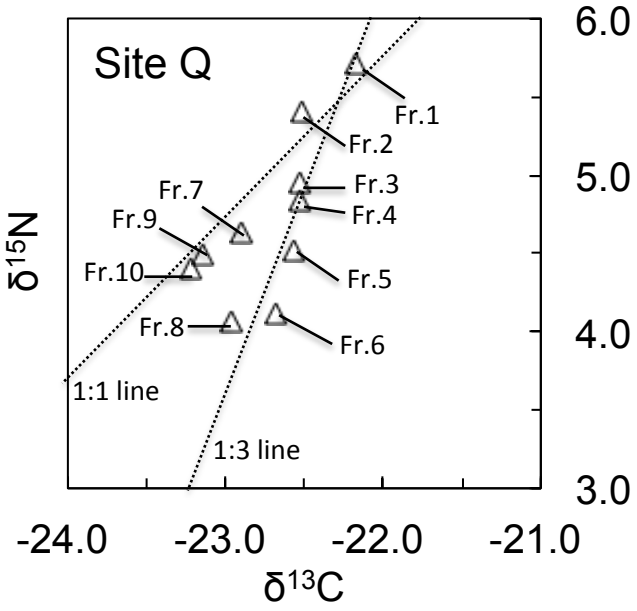
Site Q
Fr.1
Fr.2
Fr.3
Fr.4
Fr.5
Fr.6
Fr.7
Fr.8
Fr.9
Fr.10
1:1 line
1:3 line
δ15N
δ13C
6.0
5.0
4.0
3.0
-24.0
-23.0
-22.0
-21.0

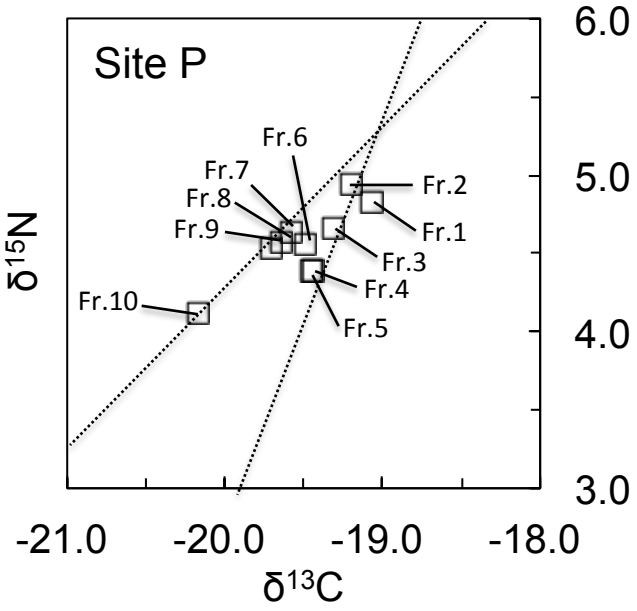
Site P
Fr.1
Fr.2
Fr.3
Fr.4
Fr.5
Fr.6
Fr.7
Fr.8
Fr.9
Fr.10
δ15N
δ13C
6.0
5.0
4.0
3.0
-21.0
-20.0
-19.0
-18.0

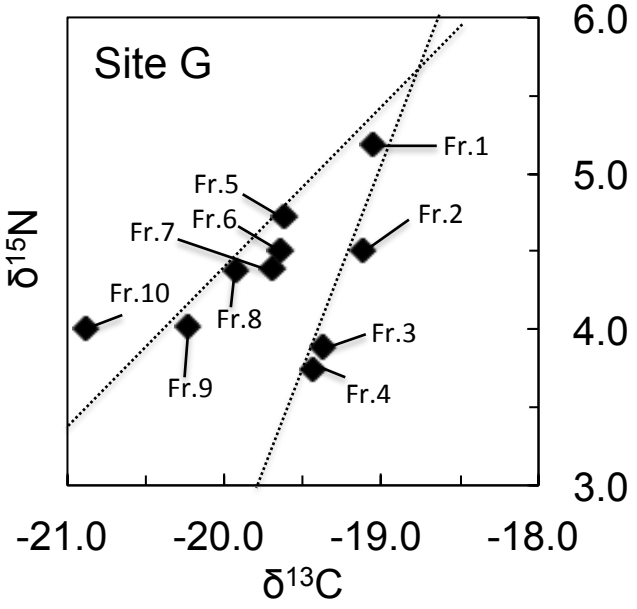
Site G
Fr.1
Fr.2
Fr.3
Fr.4
Fr.5
Fr.6
Fr.7
Fr.8
Fr.9
Fr.10
δ15N
δ13C
6.0
5.0
4.0
3.0
-21.0
-20.0
-19.0
-18.0

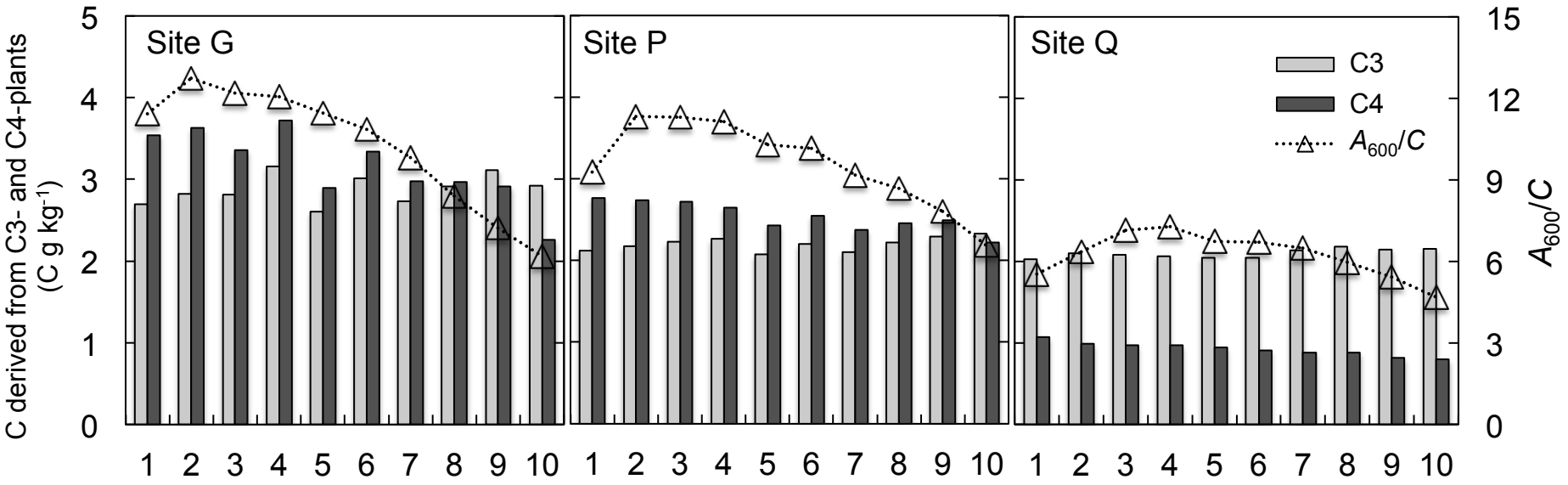
Site G
Site P
Site Q
C3
C4
A_{600}/C
C derived from C3- and C4-plants (C g kg^{-1})
A_{600}/C
0
1
2
3
4
5
0
3
6
9
12
15
1 2 3 4 5 6 7 8 9 10

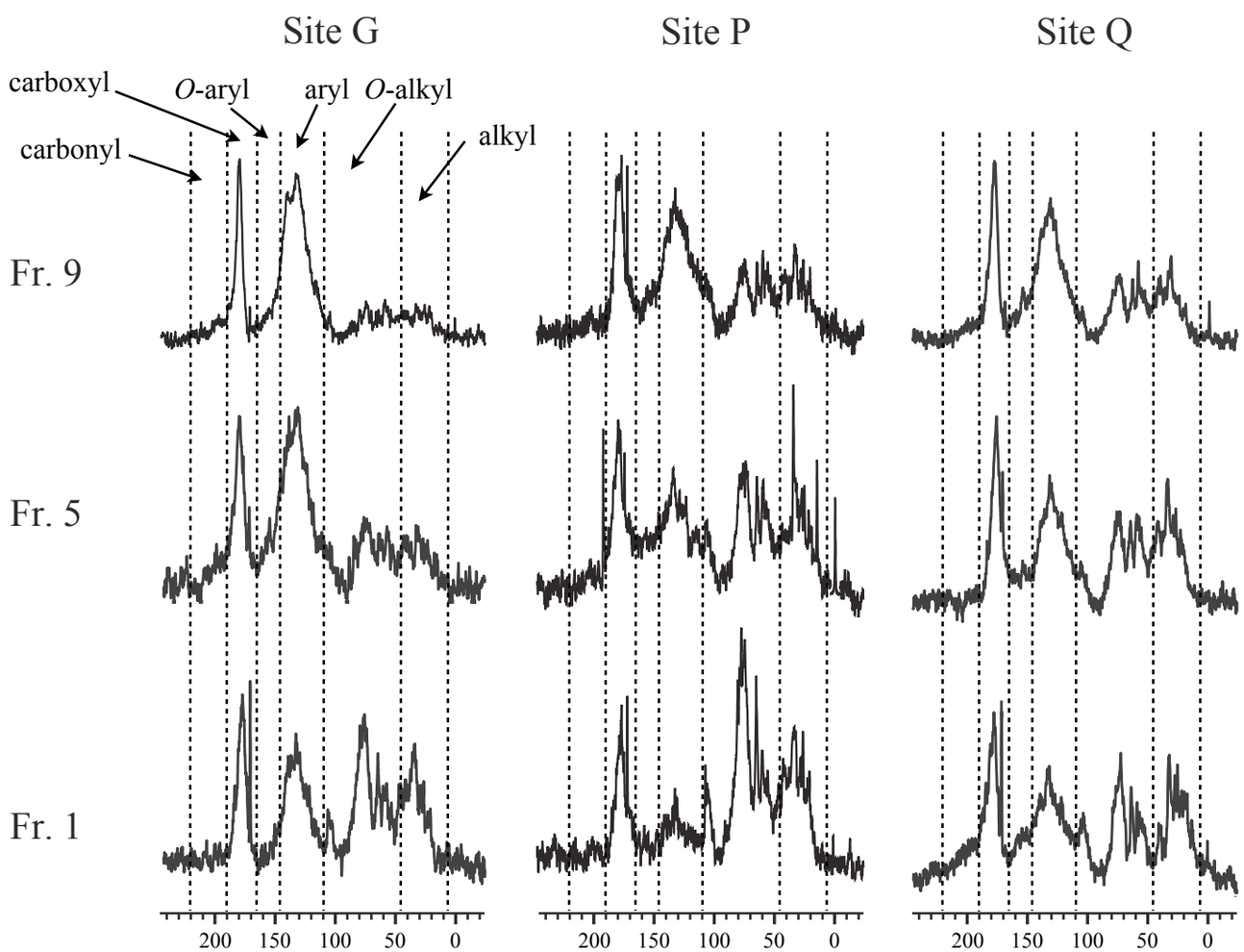
Site G
Site P
Site Q
carboxyl
O-aryl
aryl
O-alkyl
alkyl
carbonyl
Fr. 9
Fr. 5
Fr. 1
200
150
100
50
0